 Bull. Chem. Soc. Jpn., 75, 973–983 (2002)

Time-Dependent Vibration Stokes Shift during Solvation: Experiment and Theory

John B. Asbury, Yongqiang Wang, and Tianquan Lian*

Department of chemistry, Emory University, Atlanta, GA30322, USA

(Received September 7, 2001)

Peak shift dynamics of CO stretching modes of [Re(R_2-bpy)$(CO)_3$Cl] [R = COOH and COOEt] complexes in their MLCT excited state were studied in polar solvents using femtosecond visible pump and IR probe spectroscopy. For Re complex in dimethyl formamide, peak shift magnitudes for the three CO stretching modes are different but their dynamics are identical. Comparison in different alcohols showed that peak shift magnitude increases with solvent dielectric constant and peak shift time follows the trend of solvation time. The observed peak shift is attributed to solvation-induced time-dependent vibrational Stokes shift. A general theory based on the Onsager dielectric continuum model of solute solvent interaction and time-dependent reaction field was developed to qualitatively describe time-dependent vibrational Stokes shift. The theory predicts that the peak shift correlation function is determined by solvent dielectric relaxation at the vibration frequency, and the peak shift magnitudes are solvent and normal mode dependent. Although the observed trend of solvation-induced vibrational Stokes shift is consistent with the theoretical predictions, other contributions such as solute polarizability should also be included in more complete models. Solvation induced vibrational Stokes shift may be a general phenomenon in time-resolved vibrational spectroscopy of molecules undergoing significant change in charge or charge distribution.

Solvent dynamics play important roles on chemical reactions in the condensed phase.[1–4] The effects of solvent dielectric response on the static electronic spectra of solute molecules have been extensively investigated and well described by the Oshika–Lippert-Mataga equation.[5] This equation is based on Onsager dielectric continuum description of solvent–solute interaction, in which solvent is treated as a dielectric continuum and the solute as a point dipole in a spherical cavity.[6,7] This theory was later extended to describe dynamic effect of solvation on fluorescence spectra of solute molecules by van der Zwan and Hynes[8] and Bagchi, Oxtoby and Fleming.[9] A general microscopic theory that includes the effect of both vibrational relaxation and solvation on time-resolved fluorescence spectra was also developed by Loring, Yan and Mukamel.[10] The predicted time-dependent fluorescence Stokes shift (TDFSS) of solute molecules during the solvation process has been observed by many experimental studies of dye molecules in polar solvents.[2,11–20] The detailed molecular motions giving rise to the solvent response were investigated by Molecular Dynamics simulations.[13,15,21–25] Through these experimental and simulation studies, solvation dynamics and their effects on solute electronic spectral evolution in bulk solution are well understood.

The effect of solvation dynamics on the vibrational spectra of solute has not been extensively investigated. To the best of our knowledge, there have been only a few reports on this effect,[26–28] and a detailed theoretical and experimental understanding is still lacking. Time-resolved IR and Raman spectroscopy techniques have been widely used to study dynamical processes in solution,[29–33] biological systems,[34–37] and interfaces.[38–41] In many systems, such as photo-synthetic reaction center,[42] mixed valence transition metal compounds,[33,43] and dye sensitized nanomaterials,[41] significant charge redistribution occurs as a result of photoexcitation. Subsequent reorganization of the medium in response to charge change, i.e. solvation, is expected. It remains unclear how the solvation process affects the time-evolution of vibrational spectra of the solute molecules in these systems. The understanding of this effect is important for the correct assignment of vibrational spectral evolution. Furthermore, it will allow the study of solvation dynamics using time-resolved vibrational spectroscopy. This alternative approach has some unique advantages. This technique can measure solvent response with probe molecules that have no strong fluorescence but strong IR (or Raman) modes, hence providing a wider range of probe molecules for solvation study. Because it is very sensitive to specific solvent–solute interactions such as hydrogen bonding,[27,44–48] IR probe of solvation dynamics may provide molecular level understanding of solvent motion during the solvation process, which is still elusive to experimental studies.

In this paper, we present our recent study on the time evolution of solute vibrational spectra during solvation process. We observed time-dependent vibrational peak shift of CO stretching bands of [Re(R_2-bpy)$(CO)_3$Cl] [bpy = 2,2′-bipyridine, R = COOH (called ReC0), and COOEt (ReC1M)] (Scheme 1) in polar solvents. The magnitude and dynamics of the observed peak shift depend systematically on the dielectric constant and solvation time of the solvents respectively. The observed peak shift is attributed to time-dependent vibrational Stokes shift of solute molecule during the solvation process. To obtain a qualitative understanding of the time-dependent vibrational Stokes shift, we develop a simple and general theoretical model to de-

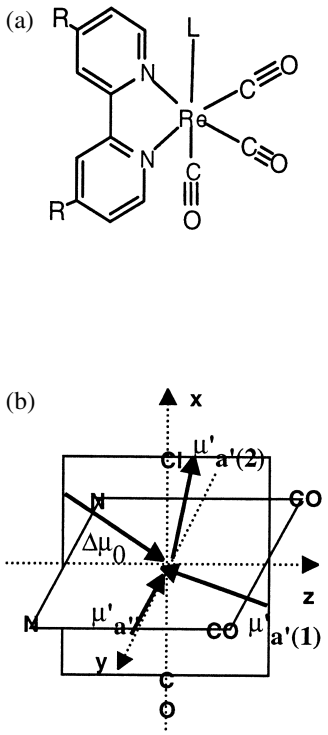

Scheme 1. (a) Structure of [Re(R_2-bpy)($CO)_3$Cl] [R = COOH (called ReC0) or COOEt (called ReC1M)]. (b) Directions of permanent dipole and dipole derivatives along the three CO stretching normal modes.

scribe the effect of solvation on vibrational spectral change of polyatomic solute molecules in polar solvents. We use the Onsager dielectric continuum model to describe solvent solute interaction. We extend Buckingham[49,50] and Pullin's[51,52] theory to account for the dynamic effect of solvation on solute vibrational spectral change. Solvation dynamics is described using the time-dependent reaction-field approach developed by van der Zwan and Hynes.[8] We consider a solute molecule with different permanent dipole moment in the ground and excited state. Photoexcitation of the solute molecule to an excited state creates a solute in a nonequilibrium solvent configuration. The theory describes the magnitude and dynamics of solute vibrational peak shift during the solvation process. A similar theoretical model was recently used to account for CO stretching mode peak shift dynamics in the S_1 excited state of coumarin 152.[28,47]

The remaining of the paper is organized as follows. In the section of Theory, we present a theory for dynamic vibrational Stokes shift of solute molecules during solvation process. In the section of Experimental and Results, experimental details and results of the femtosecond infrared study of the dynamic vibrational peak shift of [Re(R_2-bpy)Cl($CO)_3$] in polar solvents are presented. We will discuss the contribution of vibrational relaxation and solvation to the observed peak shift dynamics in section of Discussion. We will also compare the observed peak shift magnitude and dynamics with predictions of the simple theoretical model to provide an qualitative explanation and discuss other contributions.

1. Theory

i) Theory of Static Vibrational Peak Shift. The effect of solvent on the static vibrational spectra of solute has been a problem of interest for a long time. Early theoretical studies using dielectric continuum model dated back to Kirkwood.[56,57] More detailed theories were later developed by Buckingham[49,50] and Pullin.[51,52] These theories of solvent induced shift of solute static vibrational spectra are based on Onsager dielectric continuum model of solvent solute interaction.

Assume that the gas phase potential for a polyatomic molecule is given by:[51]

$$V_g(...\eta_i,...) = \frac{1}{2}\sum_i \lambda_i \eta_i^2 - \sum_{i,j,k} b_{ijk}\eta_i\eta_j\eta_k + ... \tag{1a}$$

Here η_i is the displacement along normal coordinate i and b_{ijk} is the cubic anharmonic-coupling coefficient. It is assumed that the total dipole moment of the molecule can be expanded as a function of the normal mode displacement:

$$\begin{aligned} \vec{\mu}(\eta) &= \vec{\mu}_0 + \sum_i \vec{\mu}_i'\eta_i + \sum_i \vec{\mu}_{ij}''\eta_i\eta_j \\ \vec{\mu}_i' &= \frac{\partial\vec{\mu}}{\partial\eta_i}; \qquad \vec{\mu}_{ij}'' = \frac{\partial^2\vec{\mu}}{\partial\eta_i\partial\eta_j}, \end{aligned} \tag{1b}$$

where μ_0 is the permanent dipole and η_i is displacement in normal mode i. Within the Onsager continuum model for solute-solvent interaction, the oscillating dipole leads to a normal-mode-displacement dependent oscillating reaction field, R, and solvent–solute interaction energy, U:[51]

$$\begin{aligned} \vec{R}(\eta) &= f_0\vec{\mu}_0 + f_\infty\sum_i \vec{\mu}_i'\eta_i + f_\infty\sum_i \vec{\mu}_{ij}''\eta_i\eta_j \\ f_0 &= f_\infty + f_{or}, \quad f_\infty = \frac{1}{a^3}\frac{2\varepsilon_\infty - 2}{2\varepsilon_\infty + 1}, \\ f_{or} &= \frac{1}{a^3}\left[\frac{2\varepsilon_0 - 2}{2\varepsilon_0 + 1} - \frac{2\varepsilon_\infty - 2}{2\varepsilon_\infty + 1}\right] \end{aligned} \tag{2a}$$

$$\begin{aligned} U(\eta) &= -\frac{1}{2}\vec{\mu}\vec{R} = U_0 + \sum_i U_i'(\eta)\eta_i \\ &\quad + \sum_{i,j}\frac{1}{2}U_{ij}''(\eta)\eta_i\eta_j + ... \\ U_0 &= -\frac{1}{2}f_0\vec{\mu}_0^2 \\ U_i'(\eta) &= -\frac{1}{2}(f_0 + f_\omega)\vec{\mu}_0\vec{\mu}_i' \\ U_{ij}''(\eta) &= -\left[(f_0 + f_\omega)\vec{\mu}_0\vec{\mu}_{ij}'' + f_\omega\vec{\mu}_i'\vec{\mu}_j'\right] \end{aligned} \tag{2b}$$

where ε_0 and ε_∞ are static and high frequency dielectric constants of solvent respectively. Treating the anharmonic terms and solvent–solute interaction as a perturbation to the harmonic potential and taking only the leading terms, the frequency shift can be shown to be:[49,50,52]

$$\begin{aligned} \nu_{\rm r} - \nu_{r0} &= -f_\infty \frac{\nu_{r0}}{2\lambda_{\rm r}}\left[2\vec{S}_{\rm r}\cdot\vec{\mu}_0 + \vec{\mu}_r{}'^2\right] - \frac{\nu_{r0}}{2\lambda_{\rm r}} f_{or}\vec{S}_r\cdot\vec{\mu}_0 \\ \vec{S}_{\rm r} &\equiv \sum_i \frac{6b_{irr}\vec{\mu}_i{}'}{\lambda_i} + \vec{\mu}_{rr}{}'' \end{aligned} \tag{3}$$

where, ν_{r0} and ν_r are the frequency of normal mode r in the gas and solution phase respectively.

ii) Time-Dependent Vibrational Stokes Shift. Let's now consider a time dependent experiment such as a visible pump/IR probe experiment. At $t = 0$, the excitation pulse promotes the molecule to the lowest lying excited state, which has a permanent dipole moment that is different from the ground state. We assume that the lowest excited state is far from other higher lying states. This assumption can often be satisfied with proper choice of molecules and excitation wavelength. In the theoretical treatment, we will neglect frequency shift due to vibrational relaxation within the excited state, although this effect is always present in real systems. Vibrational relaxation dynamics can be separated by studying nonpolar solvents or solvent free environment, in which solvation induced shift is much smaller. It can also be studied by examining the change of bandwidth, since cooling process also leads to band narrowing. Furthermore, its contribution can be minimized by exciting the molecule near the band origin. The contribution of vibrational cooling to the total peak shift dynamics will be discussed in the experimental section.

Photoexcitation creates the solute molecule in a different electronic state and a nonequilibrium solvent configuration. Change in electronic structure leads to an instantaneous change in its gas phase frequency from $\nu_0{}^{\rm g}$ to $\nu_0{}^{\rm e}$. There are two parts of the solvation-induced shift. The first term in Eq. 3a, contributed by the electronic part of the solvent dielectric response, is also instantaneous. The second term, resulted from the orientational contribution of the dielectric response, is not instantaneous. The time dependence of this response was elegantly treated by van der Zwan and Hynes.[8] They described this orientational part of the time-dependent reaction field $R_{or}(t)$, by a fictitious time-dependent dipole moment $\mu(t)$:

$$\begin{aligned} \vec{R}_{or}(t) &= f_{or}\vec{\mu}(t), \\ \vec{\mu}(t) &= \vec{\mu}_{g0}[1-z(t)] + \vec{\mu}_{e0}z(t) \end{aligned} \tag{4}$$

where μ_{g0} and μ_{e0} are permanent dipole moments in the ground and excited states respectively. $z(t)$ is the solvation coordinate whose value changes from 0 at the initial solvent configuration to 1 at the equilibrium solvent configuration. At $t = 0$, $z(0) = 0$, and $\mu(0) = \mu_{g0}$, the orientational part of the reaction field remains the same as that for the ground state dipole, since solvent molecules have no time to respond to the excited state dipole yet. At $t = \infty$, $z(\infty) = 1$, and $\mu(\infty) = \mu_{e0}$, the orientational part of the reaction field is determined by the dipole moment in the excited state, as the solvation process is completed.

Using time-dependent reaction field, we derive an expression for the time-dependent frequency shift in the excited state:

$$\nu_r(t) = \nu_{r0}^e - \frac{\nu_{r0}^e}{2\lambda_r} f_\infty\left[2\vec{S}_r\cdot\vec{\mu}_{e0} + \vec{\mu}_r{}'^2\right] - \frac{\nu_{r0}^e}{2\lambda_r} f_{or}\vec{S}_r^e\cdot\vec{\mu}(t) \tag{5}$$

It is more convenient to express the peak shift relative to the equilibrium position in the excited state:

$$\begin{aligned} \nu_r(t) - \nu_r(\infty) &= -\frac{\nu_{r0}^e}{2\lambda_r} f_{or}\vec{S}_r^e\cdot\Delta\vec{\mu}_0[1-z(t)] \\ \nu_r(0) - \nu_r(\infty) &= -\frac{\nu_{r0}^e}{2\lambda_r} f_{or}\vec{S}_r^e\cdot\Delta\vec{\mu}_0 \\ \Delta\vec{\mu}_0 &= \vec{\mu}_{e0} - \vec{\mu}_{g0} \end{aligned} \tag{6}$$

Similar to fluorescence stoke shift, a peak shift correlation function can also be defined:

$$c(t) \equiv \frac{\nu_r(t) - \nu_r(\infty)}{\nu_r(0) - \nu_{\rm r}(\infty)} = 1 - z(t) \tag{7}$$

As shown in Eq. 6, the solvation induced dynamic peak shift has two contributions (contained in S_r). The first term originates from the anharmonicity (b_{irr}) of the oscillator. The solvent polarization changes the equilibrium position of the oscillator, thus changing effective frequency of an anharmonic oscillator. The second term arises from terms quadratic in displacement in the solvent–solute interaction potential, which changes of the harmonic frequency of the oscillator. The first term sums over all anharmonically coupled modes. However, based on symmetry, change in equilibrium displacement can only occur in totally symmetric modes[51] and cubic anharmonicity coefficients, b_{irr}, are non-zero only if i belongs to totally symmetric modes.[58] Furthermore, this term is dominated by modes with dipole derivatives that are large in magnitude and lie along the direction of the permanent dipole moment change, as shown in Eq. 3.

The vibrational peak shift correlation function, shown in Eq. 7, is given by solvation time, $z(t)$, at the vibrational frequency. It is now well accepted that solvation dynamics measured in the optical frequency region for most solvents consist of an inertial component and multiple slower diffusive components.[59] Vibrational peak shift correlation function is expected to have similar dynamics, but they may be quantitatively different from fluorescence Stokes shifts. Within the dielectric continuum model, the solvation time is given by the longitudinal relaxation time of a dipole moment change, $z(t) = 1 - \mathrm{Exp}(-t/\tau_{\rm L})$, which is related to the Debye relaxation time, $\tau_{\rm D}$, by:[8,9,59]

$$\tau_{\rm L} = \frac{(2\varepsilon_\infty + 1)}{(2\varepsilon_0 + 1)}\tau_{\rm D} \tag{8}$$

Since the high frequency dielectric constant, or refractive index, is different at the visible and IR wavelength, the solvation time measured with vibrational peak shift can be different. It should be noted that mid-IR refractive index for most liquids is a complex function of wavelength because of resonance in numerous IR absorption bands. Therefore, a general statement regarding the differences in measured solvation times in the visible and IR regions may be difficult. Although, we have used a simple Debye liquid to illustrate the frequency dependence of solvation time, this theory does not specify an explicit

form of $z(t)$, and should be applicable to complex liquids.

The theory predicts the following trend in solvation induced vibrational Stokes shift:

1) Peak-shift correlation function is only dependent on solvent property.

2) The peak shift magnitude depends on dielectric constants of the solvent, solute dipole moment change between ground and excited states, as well as property of the normal modes.

3) The magnitude of the peak shift is proportional to vector product, $\mathbf{S}_r \bullet \Delta\boldsymbol{\mu}$, which is normal mode specific. It depends on cubic anharmonicity coefficients and the magnitude and direction of dipole derivatives of normal modes.

Experimental

Femtosecond IR Spectrometer: The femtosecond IR spectrometer used in these experiments is based on an amplified femtosecond Ti:sapphire laser system from Clark-MXR (1 kHz repetition rate at 800 nm, 100 fs pulse-width, 900 μJ/pulse). Nonlinear frequency mixing techniques are used to generate mid-infrared probe pulses and 400 nm pump pulses, the details of which have been described elsewhere.[60,61] Briefly, the 800 nm output is split into two beams at 500 and 400 μJ/pulse respectively. The 500 μJ beam is used to pump an optical parametric amplifier to generate two near-infrared pulses at about 1.5 and 1.9 μm respectively. These two pulses are then mixed in a $AgGaS_2$ crystal to generate mid-infrared light at about 5 μm wavelength. The mid-infrared probe pulse, with a bandwidth greater than 200 cm^{-1}, is dispersed into an imaging spectrograph where it is imaged onto a 32-element HgCdTe (MCT) infrared array detector. The amplified outputs of the 32 elements were measured for every laser shot at a 1 kHz repetition rate. Each element of the array averaged a 2 cm^{-1} slice of the infrared spectrum so that the total spectral region covered by the array was about 70 cm^{-1}. When desired, better (or worse) spectral resolution could be obtained by using a more (or less) dispersive grating. Transient kinetics traces at 32 wavelengths were collected simultaneously, from which transient spectra at different delay times were constructed. The other 400 μJ fundamental beam is attenuated with a variable neutral density filter and frequency doubled in a BBO crystal to make 400 nm pulses.

In all the experiments presented here, a moving solution or film sample was pumped at 400 nm light and the subsequent absorbance change was measured in the 1820 – 2200 cm^{-1} region. The diameters of the pump, with 1 to 3 μJ energy per pulse, and probe beams were 400 and 300 μm respectively. The instrument response function, i.e. the cross-correlation of the pump and probe pulses, was measured in a thin silicon wafer, in which 400 nm excitation leads to instantaneous generation of free carriers that absorbed strongly in the mid-infrared region. The typical instrument response was well represented by a Gaussian function with a FWHM of less than 200 fs.

Sample Preparations: Transition metal complexes [$Re(R_2$-bpy)$(CO)_3Cl$] [bpy = 2, 2′-bipyridine, R = COOH (called ReC0), and COOEt (ReC1M)] were chosen for the study because they have been shown to exhibit IR rigidochromic effect[53–55] and their photophysics have been well examined.[62] They are prepared according to a published procedure.[62] ReC1M and ReC0 have very similar UV-visible and IR spectra, but the former is much more soluble in alcohols. The solution sample in dimethyl formamide (DMF) was prepared by dissolving ReC0 and ReC1M to 1.8 mM concentration. The solution sample of ReC1M in alcohol has concentration of about 1 mM. Methanol (MeOH), ethanol (EtOH), 2-propanol (2-PrOH), and isobutyl alcohol (*i*-BuOH) are spectroscopy grade solvents used as received. These samples were stable for at least several days in the dark. The sample cell, with a path length of 250 μm, were scanned rapidly and/or flowed continuously in a peristaltic pump during measurements to prevent any long term photo-product build-up. The integrity of samples were checked by UV-visible and IR spectra. No noticeable degradation was observed during the course of transient absorption measurement.

Spectra Fitting: Most transient spectra shown later have been fitted to obtain peak position and width. Each ground and excited state peak is represented by a gaussian function. The position and width of the ground state peaks (bleach) and their relative amplitude are fixed as measured in FTIR spectrum. The excited state peak position, width, and amplitude are allowed to vary to obtain the best fit. Examples of the fitted spectra are shown in Fig. 4.

Results

1) ReC0 in DMF. Shown in Fig. 1 are transient IR different spectra of ReC0 in DMF at different delay times. 400 nm excitation, near the center the MLCT band, promotes an electron from the d-orbitals of Re(I) to the π^* orbital of bipyridine. The lifetimes of the MLCT excited state of similar Re complexes have been extensively studied as a model system of ET in the Marcus inverted region, and are known to be $>>$ 1ns.[62] The CO stretching modes in the excited state, at 1960, 1990 and 2070 cm^{-1}, are blue shifted from their ground state positions at 1890, 1915 and 2020 cm^{-1}. This blue shift resulted from the reduced electron density in the metal center in the MLCT excited state.[61] Similar vibrational spectra were measured for ReC1M in DMF (results not shown).

To assign the three CO stretching modes, we measured anisotropy values of the 400 nm pump— IR probe transient signal for ReC1M in DMF. The anisotropy decay curves measured at 1890, 1915 and 2020 cm^{-1} are shown in Fig. 2. The initial anisotropy values are -0.1, -0.2 and 0.35 respective-

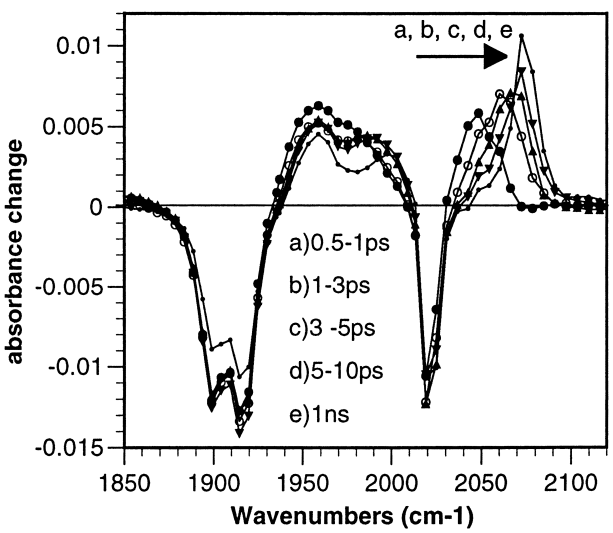

Fig. 1. Transient IR difference spectra of ReC0 in DMF at different delay time after 400 nm excitation.

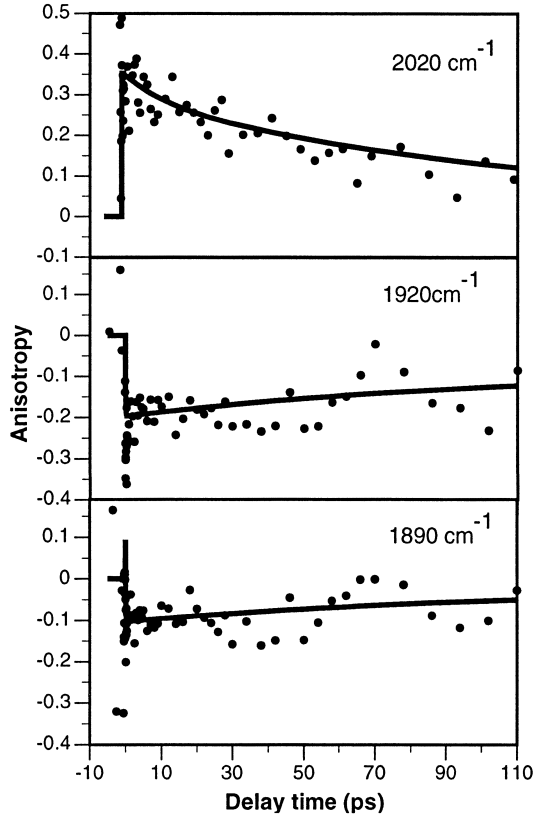

Fig. 2. Anisotropy values for bleaches of the ground state CO stretching bands of ReC1M in DMF. The solid lines are fits and solid circles are experimental data.

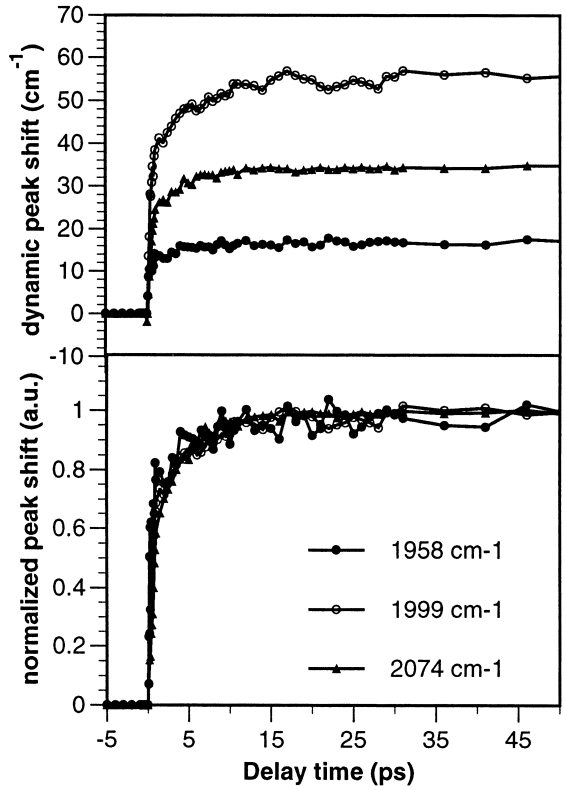

Fig. 3. Dynamic peak shift (relative to $t = 0$) of the excited state CO stretching bands of ReC0 in DMF.

ly. The initial anisotropy values for the excited state peaks at 1960, 1990 and 2070 cm^{-1} are about -0.2 ± 0.1, -0.1 ± 0.1 and 0.2. These results indicate that the highest frequency peak at 2070 cm^{-1} has a positive anisotropy value and the lower frequency peaks have negative anisotropy. Unfortunately, the poor data quality does not allow unambiguous differentiation of the two lower frequency peaks.

As shown in Fig. 1, the excited state peak positions of ReC0 in DMF shift toward high frequency with delay time. Similar blue shift was observed in ReC1M in DMF. These spectra at different delay times were fit by the procedure outlined in experimental section. The fitting result yields the peak position and width of the three excited state peaks at different delay time. Shown in Fig. 3a are the peak shift dynamics for the three peaks. The peak at 1958 cm^{-1} shows much less dynamic peak shift compared to the other two peaks. This trend is also evident in the transient spectra shown in Fig. 1. Similar mode-dependent peak-shift has been observed for ReC1M in DMF. To compare the rate of peak shift in different CO stretching bands, these three traces were normalized. As shown in Fig. 3b, their peak shift dynamics are identical within the experimental error.

2) ReC1M in Alcohols. As will be discussed later, the peak shift dynamics contains contributions from vibrational relaxation and solvation process. The solvation component should depend on solvent dynamics. Since all three CO stretching modes show same dynamics in DMF, we will compare only the high frequency mode in different solvents. This mode is chosen because it is free from spectral overlap with other two modes. ReC1M is used in this study because of its better solubility in alcohols than ReC0. Shown in Fig. 4 are the transient spectra for ReC1M in MeOH and *i*-BuOH at different delay times. The symbols are the experimental values and the solid lines are fits of the data. While the ground state positions of ReC1M in these solvents are similar, their final excited state peak positions are different. Furthermore, the time scales of peak shift are clearly different. Shown in Fig. 5 are comparisons of peak shift dynamics in MeOH, EtOH, *i*-PrOH and *i*-BuOH. The relative peak shift is shown in panel A and the normalized comparison is shown in panel B. The symbols are peak positions obtained from fitting the spectra. The peak shift is calculated relative to the position at $t = 0$. Because of limited time resolution and perturbed free induction decay signal,[63] there is large uncertainty in the peak position at $t = 0$. As a result the amount of peak shift that occurs < 100 fs were not accurately determined. These peak shift dynamics are well fitted by three-exponential functions. The fitting parameters are summarized in Table 1. The amplitude and rate of peak shift decreases from MeOH to BuOH. Peak width changes obtained from the spectral fitting are shown in Fig. 6. For ReC1M in these solvents and in DMF (result not shown) the peak width decreases with a time constant of about 4 ps, independent of solvent environment.

Discussion

1) Spectral Assignment. Both ReC0 and ReC1M have C_s

Table 1. Comparison of Peak Shift Magnitude and Dynamics in Different Solvents

Solvent	f_{or}[19]	Total shift $[\Delta\nu_T = \nu_e - \nu_g]$ / cm^{-1}	Solvation shift $[\Delta\nu_T - 20.4]$ / cm^{-1}	Dynamic shift $[\nu_e(\infty) - \nu_e(0)]$ / cm^{-1}	Fitting parameters τ_1/ps a_1	τ_2/ps a_2	τ_3/ps a_3
MeOH	0.71	37.1	16.7	20.4	< 0.1	4.3 ps	
					39%	61%	0%
EtOH	0.67	35.7	15.3	18.5	< 0.1	4.0 ps	20 ps
					22%	57%	21%
2-PrOH	0.63*	33.3	12.9	16.9	< 0.1	4.3 ps	33 ps
					24%	50%	26%
i-BuOH	0.61*	32.7	12.3	16.3	< 0.1	4.3 ps	55 ps
					18%	57%	25%
on ZrO_2		20.4	0	9.4		4.5 ps	
						100%	

*: Literature values are for 1-PrOH and 1-BuOH.

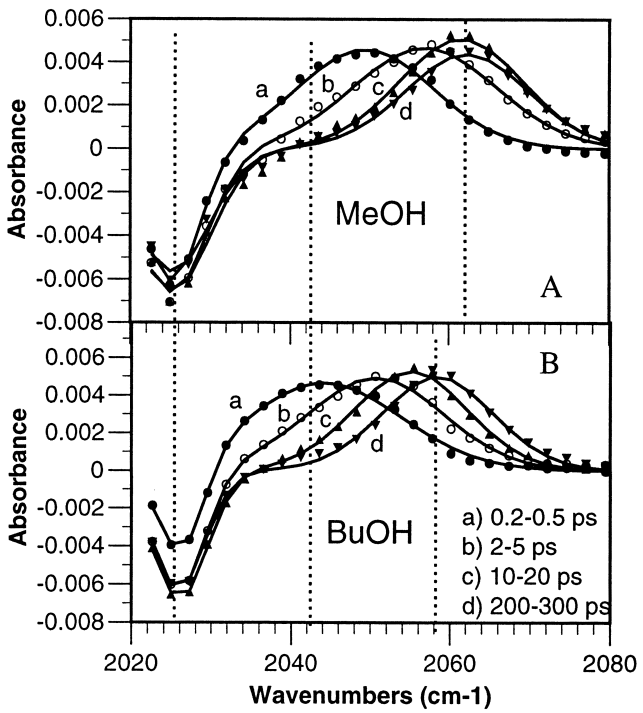

Fig. 4. Transient IR difference spectra of a′(1) mode of ReC1M in A) MeOH and B) *i*-BuOH. Symbols are experimental data and solid curves are fitted spectra.

symmetry, with three IR active CO stretching normal modes: two symmetric a′(1), a′(2) and one anti-symmetric mode a″. Normal mode analysis for a similar molecule with the same symmetry, $[Re(bpy)_2(CO)_3Cl]$[64] showed that asymmetric CO stretch mode (a″) involves only the in plane CO groups and the symmetric CO stretches involve all three CO ligands. The dipole derivative of the anti-symmetric mode lies on the *y*-axis, perpendicular to the C_s symmetry plane. The dipole derivative for both symmetric a′(1) and a′(2) modes are in the symmetry plane lying at an angle of ~28° and ~62° relative to the *z* axis respectively.[64]

The transition dipole to the MLCT excited state lies on the *z*-axis, connecting the Re atom to the center of the bipyridine ligand. The identity of the three modes and their transition dipole direction can be determined from the anisotropy values measured in the polarized 400 pump and IR probe experiment. Dipole derivatives along a normal mode determines the direction and magnitude of the IR transition dipole. From the measured anisotropy values of −0.1, −0.2 and 0.35 for the bands at 1890, 1915 and 2020 cm^{-1}, we can assign them to a′(2), a″ and a′(1) modes respectively. As expected from symmetry, a″ mode is perpendicular to the symmetry plane and the MLCT transition dipole, giving rise to an anisotropy value of −0.2. From their anisotropy values, IR transition dipoles of a′(1) and a′(2) modes lie at an angle of 22° and 73° off the *z* axis, consistent with previous normal mode analysis of a similar compound.[64] The slight difference may result from the slightly different structures of these molecules and uncertainty in the measured anisotropy values.

The excited state peaks are more difficult to assign from the anisotropy values. The molecule retains C_s symmetry in the excited state. From the positive anisotropy value, we can assign the band at 2070 cm^{-1} to that of a′(1) mode. The anisotropy values for the two low frequency bands are too noisy to distinguish. It is unclear why these anisotropy values are much smaller than those for the ground state peaks. It is interesting to note that similarly smaller excited state anisotropy values for $[Re((bpy)CO)_3Cl]$ in low temperature matrices were also observed and unaccounted for.[65] We tentatively assigned the excited state peaks at 1960 and 1990 cm^{-1} to a′(2) and a″ modes based on their corresponding position to ground state peaks at 1890 and 1915 cm^{-1}.[55] This assignment is widely used in the literature,[65] although, to the best of our knowledge, there was not any direct experimental evidence. A definitive assignment and the origin of low anisotropy values of the excited state peaks are questions for ongoing studies.

2) Vibrational Cooling. 400 nm excitation of the Re complexes to the formally ^{1}MLCT state deposits ~10,000 cm^{-1} excess energy above the lowest lying ^{3}MLCT state.[62] Strong mixing between the singlet and triplet states lead to < 100 fs intersystem crossing in related $[Ru(bpy)_3]$ complex,[66] which may be considered as relaxation within the strongly mixed MLCT manifold. We assume similar ultrafast electronic relaxation within the MLCT manifold for the Re complexes,

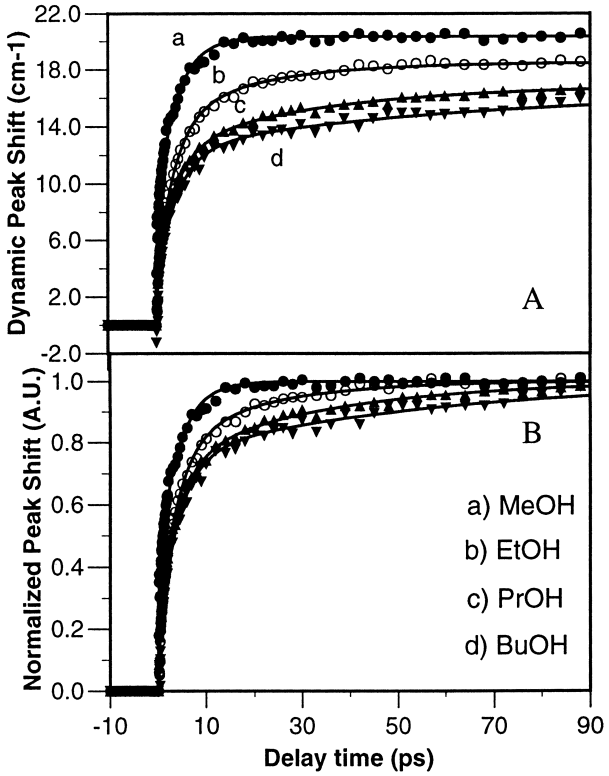

Fig. 5. A) Peak shift dynamics and B) normalized peak shift (correlation) function of the a′(1) mode of ReC1M in different alcohols. Symbols are peak position obtained from spectra fitting. Solid curves are multi-exponential fits to the peak shift data with parameters listed in Table 1.

and that the observed vibrational peak shift after the initial excitation is associated with the molecule in the lowest lying MLCT state. The effect of vibrational relaxation in the excited state needs to be understood before we can address the solvation induced peak shift. We have investigated vibrational cooling for ReC0 on ZrO_2 thin films, which we consider as a model for weakly-solvated environment. As shown previously, the initially broadened CO stretch bands undergo continuous blue shift and narrowing on the a few picosecond time scale.[61] The absorbance at the peak position of the a′(1) mode at 2069cm^{-1} was found to rise with a time constant of 1.7 ps. The measured kinetics is dependent on the probe wavelength. We have since acquired better data that allow us to fit the transient spectra to obtain peak position and width at any delay times. The analysis yielded a peak shift dynamics of the 4.5 ps and a peak width narrowing dynamics of 5 ps (result not shown). These features are strong indication of the vibration cooling process. Vibrationally hot molecules show broadened and red shifted CO stretching bands,[67] due to anharmonic coupling with low frequency modes. As the molecule cools, the CO band blue shifts and narrows.

Very similar peak width narrowing dynamics of a′(1) mode were observed for ReC1M in different alcohols as shown in Fig. 6. Peaks also narrow by about 4 cm^{-1} with time constants of 4–5 ps. These results indicate that the vibrational relaxation dynamics of modes coupled to CO stretching mode are not sensitive to the solvent environment and probably occur via

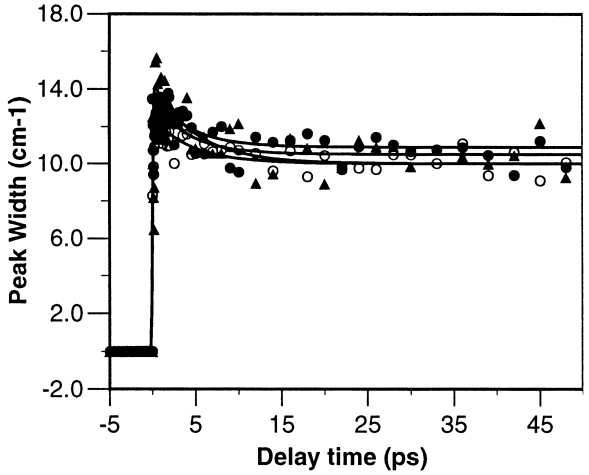

Fig. 6. Peak width narrowing dynamics of the a′(1) mode of ReC1M in different alcohols. Symbols are peak width data obtained from spectra fitting and solid curves are exponential fits.

predominantly intramolecular pathways. Therefore, we can estimate the contribution of vibrational cooling to the total peak shift by studying the molecule in a nonpolar or solvent free environment. For ReC0 on ZrO_2 films, the total shift from ground to excited state is ∼20 cm^{-1}. This value is similar to the peak shift observed for related Re carbonyl complexes in low temperature matrices[53–55] but much less than the ∼50 cm^{-1} shift observed for the same molecule in the DMF. The instantaneous part, accounting for half of the total shift, results from change of electronic structure. The subsequent dynamic shift from the initial peak position at ∼0 fs to the final position amounts to ∼10 cm^{-1}. This value can be considered as the upper limit of peak shift caused by vibrational cooling of a′(1) mode. It may contain small contribution from polarization of the ZrO_2 film and small amount of water that may be absorbed on the surface. The magnitude and dynamics of solvation induced peak shift in the solid/liquid interface are questions of great interests in ongoing studies.

3) Origin of Time-Dependent Vibrational Stokes Shift: Onsager Continuum Model. Comparison of peak shifts in low temperature matrices,[53–55] ZrO_2 films and bulk solution indicates that solvation introduces significant additional peak shift in CO stretching modes in polar solvents, which is referred to as the time-dependent vibrational Stokes shift. In fact, in DMF solution solvation induced peak shift is much larger than the estimated contribution from vibrational relaxation. The solvent dependence of peak shift magnitude and dynamics suggests that the observed peak shift is caused by the solvation response of the polar solvent. To provide insight into the origin of the time-dependent vibrational Stokes shift, we developed a simple model based on Onsager dielectric continuum model, as outlined in the section of Theory. In this section, we will compare the observed peak shift with theoretical predictions of the simple model. The limitations of the model will be discussed in the next section.

Solvent-Dependent Peak Shift: According to the theory outlined in the section of Theory, vibrational Stokes dynamics should follow the solvation time $z(t)$ in the infrared frequency

and its amplitude should follow the dielectric constant as given by Eq. 6.

The peak shift magnitude of the a′(1) CO stretching mode decreases from MeOH to EtOH, PrOH and BuOH as shown in Fig. 5A. However, the dynamics peak shift has contributions from both vibrational cooling and solvation. We assume that the 20 cm^{-1} total peak shift from ground to excited state observed for a′(1) of ReC0 on ZrO_2 film contains the contribution from electronic structure change and vibrational relaxation. It is further assumed that shift caused by these two factors is the same for ReC0 and ReC1M, and in different solvent environments. With these assumptions, the solvation induced peak shift in different solvents can be calculated by subtracting 20 cm^{-1} from the total peak shift. Shown in Table 1 are various peak shift values and the f_{or} factor from literature.[19] These f_{or} factors are calculated using refractive index values in the visible. In general, refractive index in the mid-infrared is a complex function of wavelength because of resonances in IR absorption bands. However, in regions far away from resonances, its value is only slightly smaller than those in the visible.[69] For MeOH its value changes from 1.68 at 1020 cm^{-1} to 1.08 at 1044 cm^{-1} because of a resonance at ~1030 cm^{-1}. The refractive index at 1900–2060 cm^{-1} region is ~1.328, almost identical to the value of 1.327 at 598 nm. It is interesting to note that a plot of the solvation induced shift $\Delta\nu_S$ vs f_{or} factor showed an approximately linear dependence in this narrow range of solvents. Measurement in solvents with a much wider range of f_{or} values should be carried out before a more definitive relationship can be determined. Furthermore, the absolute magnitudes of peak-shift in different solvents are still uncertain. For example the sum of solvation peak shift + vibrational cooling peak shift (9 cm^{-1}) is about 4 cm^{-1} larger than the dynamic peak shift. This could result from a under-estimate of dynamic peak shift, caused by poorly defined peak position at early time, or over-estimate of vibration cooling contribution, caused by solvation shift in the film. Nevertheless, it is clear that the magnitude of solvation induced peak shift follows the trend of decreasing f_{or} factor in these liquids, which is consistent with the theoretical prediction.

The vibrational peak shift correlation functions in these alcohols, as shown in Fig. 5B, becomes increasingly slower from MeOH to BuOH. They follow the trend of the known solvation dynamics in these solvents measured by fluorescence Stokes shift.[19] Fluorescence stoke shift correlation functions in these solvents typically contain an inertial component of sub-100 fs and slower diffusive components. They are characterized by multi-exponential functions and well documented in literatures.[19] The average correlation time, $<\tau>$, defined as the amplitude weighted sum of the exponential time constants, is 5, 16, 26, and 63 ps for MeOH, EtOH, 1-PrOH and 1-BuOH respectively. The measured IR peak shift correlation functions are also well described by multiple exponential functions with a sub-100 fs component and multiple slower components. Within the limited number of solvents studied, the measured solvation dynamics are in qualitative agreement with those measured by time dependent Stokes shift.

A quantitative comparison between the measured IR peak shift correlation and fluorescence Stokes shift is difficult because the former contains significant contribution from vibrational relaxation. As shown in Table 1, there is a 4–5 ps component in all solvent although its magnitude varies. This component includes contribution from vibrational relaxation and solvation. We have not found a reliable way to subtract the contribution of the former. In ongoing experiments, we plan to reduce the contribution from vibrational relaxation by exciting the molecule closer to its band origin. Measurements in nonpolar solvents will also help to determine more accurately the contribution of vibration relaxation induced peak shift. There is a $<$ 100 fs solvation component in all four solvents. Its time constant and relative amplitude to the total shift is not accurately determined because of the lack of time resolution.

This work was motivated by recent microsecond time-resolved infrared studies of excited state dynamics of transition metal complexes.[53–55] It was observed that CO stretch bands peak shifts in the ^{3}MLCT excited state of [Re(bpy)Cl(CO)$_3$] are much larger in fluid solutions than in low temperature matrices. This effect, called IR rigidochromism, was attributed to reduced solvation responses of frozen matrices because their rotation motion was restricted. In this study, we directly resolve the CO stretching mode peak shift dynamics of [Re(R$_2$-bpy)Cl(CO)$_3$] [R = COOH or COOEt] in polar solvents during the solvation process. The observed trend can also be used to explain the IR rigidochromic effect observed for [Re(bpy)-Cl(CO)$_3$] in low temperature matrices.[53–55] In frozen matrices, the solvent molecules can not undergo reorientation motion. The reduced peak shift in matrices can be attributed to the lack of the orientational solvation contribution to the total peak shift.

Mode-Dependence. One of unique aspect of vibrational Stokes shift is the normal mode dependence of peak shift magnitude. As shown in Eq. 6 the magnitude of the shift is dependent on the vector product, $\boldsymbol{S_r \cdot \Delta\mu}$ of mode specific parameter S_r and the dipole moment change, while the peak shift correlation function are mode independent. As shown in Figs. 1 and 3, the magnitude of peak shift is dependent on the normal modes, consistent with the theoretical expectation. Furthermore, the normalized peak shift dynamics (i.e. the correlation function) in different modes are identical within the experimental error (Fig. 3b) also in agreement with the theory.

The $\boldsymbol{S_r \cdot \Delta\mu}$, term can be further simplified in many cases.[51] For [Re(dcbpy)(CO)$_3$Cl], both the ground and excited state permanent dipoles lie in the C_s symmetry plane. Although the exact magnitude and direction are not well determined,[68] the vector of dipole moment change, $\Delta\mu_0$, should lie in the symmetry plane, as shown in Fig. 1b. The dipole derivatives along these normal modes are indicated by arrows in Fig. 1b.[64] For simplicity, we assume that CO stretching modes are the dominating modes in the anharmonic coupling term because of their strong oscillator strength. For convenience, we designate $\nu_1 = a'(1)$, $\nu_2 = a'(2)$, and $\nu_3 = a''$. The mode specific parameters $\boldsymbol{S_r \cdot \Delta\mu}$ are given by:

$$\begin{aligned}
\vec{S}_1 \cdot \Delta\vec{\mu} &= \frac{6b_{111}}{\lambda_1}\vec{\mu}_1{}' \cdot \Delta\vec{\mu} + \frac{6b_{211}}{\lambda_2}\vec{\mu}_2{}' \cdot \Delta\vec{\mu} + \vec{\mu}_{11}{}'' \cdot \Delta\vec{\mu} \\
\vec{S}_2 \cdot \Delta\vec{\mu} &= \frac{6b_{122}}{\lambda_1}\vec{\mu}_1{}' \cdot \Delta\vec{\mu} + \frac{6b_{222}}{\lambda_2}\vec{\mu}_2{}' \cdot \Delta\vec{\mu} + \vec{\mu}_{22}{}'' \cdot \Delta\vec{\mu} \qquad (9) \\
\vec{S}_3 \cdot \Delta\vec{\mu} &= \frac{6b_{133}}{\lambda_1}\vec{\mu}_1{}' \cdot \Delta\vec{\mu} + \frac{6b_{233}}{\lambda_2}\vec{\mu}_2{}' \cdot \Delta\vec{\mu}
\end{aligned}$$

μ_{33}''lies along y axis and its vector products with permanent dipole moment change[68] is zero. It has been estimated that peak shift may be dominated by the anharmonicity terms.[51,52] In that case, the above equations can be further simplified.

It should be emphasized here that the peak shift direction and magnitude of each mode is determined by dipole derivative of all modes it coupled to and the coupling coefficients as shown in Eq. 9. To quantify the difference in the peak shift for different modes, the values of the anharmonic coupling coefficients, dipole derivatives and vector of permanent dipole moment change are needed. Many of these parameters are not available for the Re complexes. In molecules with higher symmetry, the orientations of permanent dipole moments in ground and excited state are more uniquely determined. The dipole derivative is directly related to the oscillator strength and can be readily obtained. The cubic anharmonicity coefficients are more difficult to obtain. These parameters may be obtainable in molecules with fewer CO groups. Future experiments will explore more quantitative aspects of the theoretical prediction.

4) Origin of Time-Dependent Vibrational Stokes Shift: Contribution of Solute Polarizability. The simple theoretical model based on non-polarizable solute in dielectric continuum of solvent predicts trends that are consistent with the observed peak shifts in CO stretching modes in Re complexes. This model provided a simple qualitative explanation of the time-dependent vibrational Stokes shift. More quantitative analysis requires full consideration of all contributions, which are beyond the simple analytical formula shown in the section of Theory. For example, this theory neglects the contribution of solute polarizability. The time-dependent reaction field polarizes the solute, increasing its dipole moment, which in turn changes the reaction field. Polarizability has been shown to have non-negligible effect on fluorescence stoke shift even within the continuum model.[9] The effect of polarizability on the static vibrational spectra of solute has been formulated.[49–52] However, rigorous incorporation of polarizability in the time-dependent fluorescence Stokes shift expression was shown to be difficult.[9] Same difficulty exists in including solute polarizability in the theory of dynamics vibrational peak shift. The contribution of polarizability to solute dipole moment and fluorescence stoke shift has been examined by molecular dynamics simulations.[22,70,71] It was found that solute polarizability changes the structure of the solvation shell and decreases the solvation rate.[22,70] The solvation-induced change of solute charge distribution can be particularly significant in charge transfer complexes.[71]

In Re complexes, the excited state is a MLCT state, in which electron is moved from the Re d orbital to the π^* orbital of bipyridine ring. It is quite possible that in a polar solvent, solvation can lead to a large change in charge distribution in the ^{3}MLCT state. This can affect the CO stretching frequency by two mechanisms. The first mechanism is a direct electronic effect, in which solvation-induced change of charge distribution affects CO bond strength directly. Because of the metal center to ligand dπ–π^* back bonding, CO stretching frequency is sensitive to charge density on the metal center. In the Re complexes, the metal dπ orbitals are also mixed with the π^* orbitals of bipyridine. Increasing the electron withdrawing ability of the R group on the bipyridine ring increases the dπ–π^*(bpy) and decreases the dπ–π^*(CO) back donation, leading to an increase in the CO stretching frequency.[62] This orbital mixing was also shown in recent calculation of a related Ru complex.[72] Solvation induced change in the charge distribution in the π^* orbital of bpy or Re center will lead to a direct change in CO stretching frequency. In the second mechanism, solvation leads to dipole moment change of the polarizable solute, which affects the solvation induced vibration peak shift through the interaction of oscillating dipole with the reaction field, as outlined in the theory section. It should be pointed out that these alternative mechanisms are also induced by the solvation process, and will be solvent dependent. However, the dependence is more difficult to quantify through a simple theory. It is quite likely that all three effects contribute to the overall shift. Their relative contributions remain to be more carefully examined in future studies of simpler systems.

Conclusion

Ultrafast dynamics of $Re(CO)_3Cl(R_2\text{-bpy})$ [R = COOH and COOEt] complexes in ^{3}MLCT excited state were studied using sub-picosecond visible pump/IR probe spectroscopy. Time-dependent peak shifts in CO stretching modes were observed in polar solvents. The magnitudes of the peak shifts in DMF are different in three CO stretching modes, while their peak shift dynamics are similar. The observed peak shifts in DMF and alcohols are dominated by solvation induced peak shift, i.e. the time-dependent vibrational Stokes shift, although there is non-negligible contribution from vibrational relaxation. The latter was studied on ZrO_2 thin films, in which the molecule is at best weakly solvated. The magnitude and dynamics of the peak shift are solvent dependent. For the four alcohol solvents studied, the magnitude decreases from MeOH, EtOH, PrOH and BuOH while the rate decreases from MeOH to BuOH. The peak shift magnitude varies approximately linearly with the f_{or} factor in the limited solvent range. The observed peak shift dynamics agree with the trend of known solvation time in these solvents, but a quantitative comparison was hindered by the contribution from vibrational cooling dynamics.

To explain the origin of time-dependent vibrational Stokes shift, a general theory based on dielectric continuum model was developed. We extended the theory of static vibrational peak shift by Buckingham[49,50] and Pullin[51,52] to account for the dynamic solvation effect. In this model, the solute molecule was modeled as a non-polarizable point dipole in a spherical cavity embedded in the solvent dielectric continuum. The solute vibrational motion leads to oscillating terms in solvent-solute interaction that are dependent on normal mode displacements. The solvation process was incorporated using the time-dependent reaction field developed by ver der Zwan and Hynes.[8] The resulting theory predicts that the peak shift correlation time is determined by the dynamics of solvent dielectric relaxation in the vibration frequency and the magnitude of peak shift is dependent on solvent and normal mode.

The qualitative trend of the observed vibrational Stokes shift dynamics is consistent with the predictions of the theoretical model. However, quantitative comparison has yet to be carried out. There are other contributions to the observed dynamics. The polarizability of the solute molecule may affect the peak

shift dynamics directly by changing the charge density on Re center and indirectly by changing the dipole moment in the excited state. More works are needed to quantify the contribution from each process. It appears that polar solvation can lead to significant vibrational peak shift of solute molecules when there is large change of charge or charge distribution upon excitation. It should be a general phenomenon in time-resolved vibrational spectroscopy.

This work is supported by the National Science Foundation CAREER award under grant No. 9733796. We also would like to acknowledge the partial financial support by the Petroleum Research Fund, administered by the ACS and the Emory University Research Committee.

References

1 "Activated barrier crossing: application in physics, chemistry and biology," ed by G. R. Fleming and P. Hanggi, World Scientific Publishing Co., (1993).
2 P. F. Barbara, G. C. Walker, and T. P. Smith, *Science*, **256**, 975 (1992).
3 P. F. Barbara, T. J. Meyer, and M. A. Ratner, *J. Phys. Chem.*, **100**, 13148 (1996).
4 J. T. Hynes, in "Theory of Chemical Reaction Dynamics, Vol. IV," ed by M. Baer, CRC Press, Boca Raton (1985), pp. 171.
5 N. Mataga, Y. Kaifu, and M. Koizumi, *Bull. Chem. Soc. Japan*, **29**, 465 (1956).
6 L. Onsager, *J. Am. Chem. Soc.*, **58**, 1486 (1936).
7 C. J. F. Bottcher, "Theory of Electric Polarisation," Elsevier Publishing Company (1952).
8 G. van der Zwan and J. T. Hynes, *J. Phys. Chem.*, **89**, 4181 (1985).
9 B. Bagchi, D. W. Oxtoby, and G. R. Fleming, *Chem. Phys.*, **86**, 257 (1984).
10 R. F. Loring, Y. J. Yan, and Mukamel, *J. Chem. Phys.*, **87**, 5840 (1987).
11 P. F. Barbara and W. Jarzeba, *Adv. Photochem.*, **15**, 1 (1990).
12 R. Jimenez, G. R. Fleming, P. V. Kumar, and M. Maroncelli, *Nature*, **369**, 471 (1994).
13 S. J. Rosenthal, R. Jimenez, G. R. Fleming, P. V. Kumar, and M. Maroncelli, *J. Mol. Liq.*, **60**, 25 (1994).
14 S. J. Rosenthal, X. L. Xie, M. Du, and G. R. Fleming, *J. Chem. Phys.*, **95**, 4715 (1991).
15 M. Maroncelli and G. R. Fleming, *J. Chem. Phys.*, **88**, 5044 (1988).
16 R. M. Stratt and M. Maroncelli, *J. Phys. Chem.*, **100**, 12981 (1996).
17 J. Gardecki, M. L. Horng, A. Papazyan, and M. Maroncelli, *J. Mol. Liq.*, **65**, 49 (1995).
18 C. F. Chapman, R. S. Fee, and M. Maroncelli, *J. Phys. Chem.*, **99**, 4811 (1995).
19 M. L. Horng, J. A. Gardecki, A. Papazyan, and M. Maroncelli, *J. Phys. Chem.*, **99**, 17311 (1995).
20 E. W. Castner, Jr. and M. Maroncelli, *J. Mol. Liq.*, **77**, 1 (1998).
21 A. Papazyan and M. Maroncelli, *J. Chem. Phys.*, **102**, 2888 (1995).
22 P. V. Kumar and M. Maroncelli, *J. Chem. Phys.*, **103**, 3038 (1995).
23 M. Maroncelli, *J. Chem. Phys.*, **94**, 2084 (1991).
24 A. Papazyan and M. Maroncelli, *J. Chem. Phys.*, **95**, 9219 (1991).
25 M. Maroncelli, *J. Mol. Liq.*, **57**, 1 (1993).
26 J. B. Asbury, Y. Wang, and T. Lian, *Springer Ser. Chem. Phys.*, **66**, 554 (2001).
27 E. T. J. Nibbering and T. Elsaesser, *Appl. Phys. B*, **71**, 439 (2000).
28 E. T. J. Nibbering, C. Chudoba, and T. Elsaesser, *Isr. J. Chem.*, **39**, 333 (1999).
29 J. C. Owrutsky, D. Raftery, and R. M. Hochstrasser, *Annu. Rev. Phys. Chem.*, **45**, 519 (1994).
30 D. Raftery, R. J. Sension, and R. M. Hochstrasser, in "Activated Barrier Crossing," ed by G. R. Fleming and P. Hanggi, World Scientific (1993), pp. 163–205.
31 A. Tokmakoff and M. D. Fayer, *Acc. Chem. Res.*, **28**, 437 (1995).
32 D. D. Dlott, *Chem. Phys.*, **266**, 149 (2001).
33 S. K. Doorn, R. B. Dyer, P. O. Stoutland, and W. H. Woodruff, *J. Am. Chem. Soc.*, **115**, 6398 (1993).
34 R. M. Hochstrasser, *J. Chem. Educ.*, **75**, 559 (1998).
35 M. Lim, T. A. Jackson, and P. A. Anfinrud, *Science*, **269**, 962 (1995).
36 K. D. Rector, J. R. Engholm, C. W. Rella, J. R. Hill, D. D. Dlott, and M. D. Fayer, *J. Phys. Chem. A*, **103**, 2381, (1999).
37 R. B. Dyer, K. A. Peterson, P. O. Stoutland, and W. H. Woodruff, *Biochemistry*, **33**, 500 (1994).
38 G. L. Richmond, *Annu. Rev. Phys. Chem.*, **52**, 357 (2001).
39 G. L. Richmond, *Anal. Chem.*, **69**, 536A (1997).
40 E. J. Heilweil, M. P. Casassa, R. R. Cavanagh, and J. C. Stephenson, *Annu. Rev. Phys. Chem.*, **40**, 143 (1989).
41 J. B. Asbury, E. Hao, Y. Wang, H. N. Ghosh, and T. Lian, *J. Phys. Chem. B*, **105**, 4545 (2001).
42 S. Maiti, G. C. Walker, B. R. Cowen, R. Pippenger, C. C. Moser, P. L. Dutton, and R. M. Hochstrasser, *Proc. Nat. Acad. Sci. U. S. A.*, **91**, 10360 (1994).
43 C. Wang, B. K. Mohney, R. D. Williams, V. Petrov, J. T. Hupp, and G. C. Walker, *J. Am. Chem. Soc.*, **120**, 5848 (1998).
44 J. Stenger, D. Madsen, J. Dreyer, E. T. J. Nibbering, P. Hamm, and T. Elsaesser, *J. Phys. Chem. A*, **105**, 2929 (2001).
45 E. T. J. Nibbering, F. Tschirschwitz, C. Chudoba, and T. Elsaesser, *J. Phys. Chem. A*, **104**, 4236 (2000).
46 C. Chudoba, E. T. J. Nibbering, and T. Elsaesser, *J. Phys. Chem. A*, **103**, 5625 (1999).
47 C. Chudoba, E. T. J. Nibbering, and T. Elsaesser, *Phys. Rev. Lett.*, **81**, 3010 (1998).
48 W. T. Grubbs, T. P. Dougherty, and E. J. Heilweil, *J. Phys. Chem.*, **99**, 10716 (1995).
49 A. D. Buckingham, *Proc. R. Soc. London, A*, **255**, 32 (1960).
50 A. D. Buckingham, *Proc. R. Soc. London, A*, **248**, 169 (1958).
51 A. D. E. Pullin, *Spectrochim. Acta*, **13**, 125 (1958).
52 A. D. E. Pullin, *Proc. R. Soc. London, A*, **255**, 39 (1960).
53 M. W. George and J. J. Turner, *Coord. Chem. Rev.*, **177**, 201 (1998).
54 I. P. Clark, M. W. George, and J. J. Turner, *J. Phys. Chem. A*, **101**, 8367 (1997).
55 I. P. Clark, M. W. George, F. P. A. Johnson, and J. J. Turner, *Chem. Commun.*, **1996**, 1587.
56 W. West and R. T. Edwards, *J. Chem. Phys.*, **5**, 14 (1937).
57 J. G. Kirkwood, *J. Chem. Phys.*, **2**, 351 (1934).

58 E. B. Wilson Jr., J. C. Decius, and P. C. Cross, "Molecular vibrations: the theory of infrared and Raman vibrational spectra," Dover publications, Inc., New York (1955).
59 M. Maroncelli and G. R. Fleming, *J. Chem. Phys.*, **86**, 6221 (1987).
60 H. N. Ghosh, J. B. Asbury, and T. Lian, *J. Phys. Chem. B*, **102**, 6482 (1998).
61 Y. Wang, J. B. Asbury, and T. Lian, *J. Phys. Chem. A*, **104**, 4291 (2000).
62 L. A. Worl, R. Duesing, P. Chen, L. D. Ciana, and T. J. Meyer, *J. Chem. Soc., Dalton Trans.*, **1991**, 849.
63 T. Lian, S. E. Bromberg, M. Asplund, H. Yang, and C. B. Harris, *J. Phys. Chem.*, **100**, 11994 (1996).
64 D. R. Gamelin, M. W. George, P. Glyn, F. W. Grevels, F. P. A. Johnson, W. Klotzbucher, S. L. Morrison, G. Russell, K. Schaffner, and J. J. Turner, *Inorg. Chem.*, **33**, 3246 (1994).
65 M. J. Clark, Ph. D. thesis, University of Nottingham (1997).
66 N. H. Damrauer, G. Cerullo, A. Yeh, T. R. Boussie, C. V. Shank, and J. K. McCusker, *Science*, **275**, 54 (1997).
67 T. P. Dougherty and E. J. Heilweil, *Chem. Phys. Lett.*, **227**, 19 (1994).
68 F. W. M. Vanhelmont and J. T. Hupp, *Inorg. Chem.*, **39**, 1817 (2000).
69 J. E. Bertie, S. L. Zhang, H. H. Eysel, S. Baluja, and M. K. Ahmed, *Appl. Spectrosc.*, **47**, 1100 (1993).
70 F. Chicos, R. Brown, and P. A. Bopp, *J. Chem. Phys.*, **114**, 6834 (2001).
71 T. Ishida and P. J. Rossky, *J. Phys. Chem. A*, **105**, 558 (2001).
72 Y. G. K. Shin, B. S. Brunschwig, C. Creutz, M. D. Newton, and N. Sutin, *J. Phys. Chem.*, **100**, 1104 (1996).